Nigerian Journal of Physics (NJP)
ISSN online: 3027-0936
ISSN print: 1595-0611
DOI: https://doi.org/10.62292/njp.v33i3.2024.268
Volume 33(3), September 2024

Analysis of Vibrational Resonance in a Biophysical System

[1,2]Olonade, K. O., *[1]Roy-Layinde, T. O., [1]Oyero, B. A., [3]Omoteso, K. A., [1]Odunaike, R. K. and [1]Laoye, J. A.

[1]Department of Physics, Olabisi Onabanjo University, Ago-Iwoye, Nigeria
[2]Department of Science Laboratory Technology, Moshood Abiola Polytechnic, Ojere, Abeokuta, Nigeria.
[3]Department of Electrical and Electronic Engineering, University of Derby, Markeaton Street, Derby, United Kingdom

*Corresponding author's email: roy-layinde.taiwo@oouagoiwoye.edu.ng

ABSTRACT

Living systems are composed of molecules and atoms that can exhibit specific quantum effects, including coherent electric vibration, and vibrating systems that undergo resonance. Due to their resonance, biological materials can transfer energy when they vibrate at a specific frequency. In this paper, we establish the occurrence of vibrational resonance in a biophysical system modeling activated enzyme molecules in the brain waves. The VR was characterised using the response amplitude, Q which was numerically calculated using the Fourier coefficient of the output signal. The external high-frequency signal affected the enzyme-substrate reaction and amplified the combination process observed at resonance. Importantly, double resonances were induced by the strength of the decay rate. Resonance, induced by the strength of the decay rate and the external high-frequency signal would lead to significant brain wave activity related to inherent energy transfers from changes to the decay rate, and enzyme-substrate combination, and could be observed from the Electroencephalogram.

Keywords:
Enzyme,
Biophysical system,
Vibrational resonance.
Response amplitude,
Substrate.

INTRODUCTION

The origin of the cosmos is energy, a form formed from nothingness whose principle of activity is manifested via change under the control of entropy. Matter is an asymmetric kind of light that can interact and absorb energy, molding and creating things like living cells. A symmetric energy state is necessary for the grouping of fundamental particles that make up a live cell. The key to comprehending the concept of consciousness lies in the extremely conserved energy found in electromagnetic radiation. When these natural forces cause highly ordered things to vibrate at their inherent frequency or at frequencies that occur naturally, resonating frequencies are created. Due to their resonance, bodies and cells can transfer energy between domains, resulting in a continuous state of interference and interaction that maintains the connectivity of the whole universe (Pereira, 2015).

Newton's laws of motion serve as the foundation for the mathematical explanation of physical systems' motion. In explaining the dynamics of physical systems within classical boundaries, Newton's equations of motion emphasize the relationship underlying every force acting on a body and the resulting motion. When representing continuous changes in a variety of physical properties during motion, the differential equation (DE) has shown to be a helpful tool. DE simulates real-world deterministic and stochastic processes seen in engineering, biology, and the physical sciences. A linear differential equation is a reasonable approximation of a nonlinear system in the premise of any dynamic or static solution that is tenable to an appropriate perturbation process (Roy-Layinde et al., 2020). It explains sufficiently modest oscillations in a smooth dynamical system. Since the oscillations in most real-world systems are neither smooth nor tiny, nonlinear differential equations are a better fit for modeling these systems.

Resonance is the term used to describe the improved response of a system when the frequency of an external driving force coincides with its natural frequency. The Enhancement of a low-frequency (LF) nonlinear system to give a maximum response, brought about by an external stimulus is characterised as nonlinear resonances. Based on the sort of external force acting on the system, the enhancement produces many types of resonance: coherence resonance, vibrational resonance, ghost resonance, chaotic resonance, autoresonance, and

stochastic resonance (Rajasekar and Sanjuan, 2016). Vibrational resonance (VR) is produced when a high-frequency (HF) periodic signal is substituted for noise (Roy-Layinde et al., 2024). VR is helpful in the identification of weak signals and the dampening of undesired signals in systems (Vincent et al., 2021; Yang et al., 2024).

Research on vibrational resonance in systems with monostable (Jeyakumari et al., 2009b), bistable (Gitterman, 2001; Chizhevsky and Giacomelli, 2006; Yao and Zhan, 2010) and multistable potentials (Yang and Liu, 2010; Rajasekar et al., 2011; Chizhevsky, 2014; Roy-Layinde et al., 2017; Vincent et al., 2018) has grown dramatically over the last 20 years. The VR phenomenon has been used to understand physical processes in mechanical oscillators (Jeyakumari et al., 2009a, 2011), information (Pan et al., 2021) and image processing (Morfu et al., 2021), plasma (Roy-Layinde et al., 2016), bubble (Omoteso et al., 2021), laser (Chizhevsky, 2021), neuron (Yu et al., 2011; Calim et al., 2021), gyroscope (Oyeleke et al., 2021; Sahoo and Chatterjee, 2021), quantum systems (Olusola et al., 2020; Paul and Shankar Ray, 2021) and fractional-order systems (Qin et al., 2017; Yan et al., 2018).

Since the introduction of the coherent oscillation in biophysical systems considered in this research through the case of an enzymatic substrate reaction with ferroelectric behavior in brain waves model, just few aspects of its dynamics have been employed. Based on this, this article intends to study VR in a biophysical system modelling activated enzyme molecules in brain wave.

Model Description

A second order non-autonomous differential equation representing activated enzyme molecules in brain waves serves as the biophysical model in this work. The model is based on long range coherence interactions which can initiate specific chemical reactions and transport processes in enzymes (Fro¨hlich, 1968). Kadji et al. (2007) considers the biological model as a combination of the enzyme-substrate reaction together with the ferroelectric behaviour with *S* substrate molecules with *N* and *Z* representing the population of excited enzymes and unexcited enzymes, respectively. The number of substrates S, the concentration Z of the remaining unexcited enzymes, and the rate of rise of the activated enzymes were considered to be proportionate to N, S, and Z, respectively, in the system of nonlinear differential equations.

$$\frac{dN}{d\tau} = \nu NZS - \xi N, \quad (1a)$$

$$\frac{dS}{d\tau} = \gamma S - \nu NZS, \quad (1b)$$

$$\frac{dZ}{d\tau} = \xi N - \nu NZS - \lambda(Z - C), \quad (1c)$$

where γ is the range of the attraction of the substrate particles initiated by spontaneous catalytic reactions, v is the nonlinear enzyme-substrate reaction strength and the rate at which excited enzymes decay to the ground (or weakly polar) state is ξ. The value of λ (Z − C) is derived from the long-range interaction, where C denotes the equilibrium amount of molecules of unexcited enzymes in the absence of both substrate and excited enzyme, or N = S = 0. A dimensionless biophysical system of the following form is obtained by taking into account the system's intrinsic resistance to ferroelectric tendency, potential external chemical fluctuations, or contributions to the electric field F from fluctuations in temperature and an externally applied field on the excited enzyme. For small values of excess amounts of activated enzymes ε and substrate η, the combined dielectric and chemical contribution results in:

$$\ddot{x} - \mu(1 - x^2 + \alpha x^4 - \beta x^6)\dot{x} + x = f\cos\omega t, \quad (2)$$

where the dots denote differentiation w.r.t time. α and β are positive coefficients of higher order nonlinearities in damping parameter, μ is the amplitude of damping coefficients, and while ω and f denote the frequency and amplitude of the externally applied input signal respectively.

It has been demonstrated that the biophysical system governed by Equation (2) displays a wide range of dynamical behavior, including chaotic, quasiperiodic, and periodic oscillations (Kaiser, 1981a,b; Kaiser and Eichwald, 1991; Kadji et al., 2007; Roy-Layinde et al., 2020).

To study VR, a fast periodic signal of the form $g\cos\omega t$, is coupled with the weak external driving signal, so the biharmonically driven form of Equation (2) is given by

$$\ddot{x} - \mu(1 - x^2 + \alpha x^4 - \beta x^6)\dot{x} + x = f\cos\omega t + g\cos\Omega t, \quad (3)$$

Where Ω and g are the frequency and amplitude of the high-frequency external periodic signal.

MATERIALS AND METHOS

First, we obtain the output signal by numerically solving Equation (3) using the Fourth-order Runge-Kutta (FORK) Scheme (FORK). The FORK algorithm is applied to a coupled first-order Ordinary Differential Equations (ODEs) which are obtained by first re-writing Equation (3) in the form:

$$\frac{dx}{dt} = y \quad (4a)$$

$$\frac{dy}{dt} = \mu(1 - x^2 + \alpha x^4 - \beta x^6)\dot{x} - x + f\cos\omega t + g\cos\Omega t. \quad (4b)$$

The response amplitude, or response factor Q, is commonly employed to describe resonance. It offers an understanding of the process by which an amplified output is produced by modulating the characteristics of a high-frequency signal connected to a nonlinear system that is weakly driven. Usually, the output signal's

Fourier spectrum is used to calculate the response amplitude. The reason for this is because the sum of the Fourier components of any periodic function may be used to roughly express it. Thus, the response amplitude Q may be expressed as form in terms of the Fourier sine Q_s and cosine Q_c components:

$$Q_s = \frac{2}{nT}\int_0^{nT} x(t)\sin\omega t\, dt \quad (5a)$$

$$Q_c = \frac{2}{nT}\int_0^{nT} x(t)\cos\omega t\, dt \quad (5b)$$

so that Equation (5) may then be used to calculate the amplitude, A, and phase shift, Φ given as

$$A = \sqrt{Q_s^2 + Q_c^2} \quad (6)$$

$$\Phi = \tan^{-1}\left(\frac{Q_s}{Q_c}\right), \quad (7)$$

so that, in order to calculate the response amplitude, Q,

$$Q = \frac{A}{f} = \frac{\sqrt{Q_s^2+Q_c^2}}{f}. \quad (8)$$

To generate the numerical results, Equation (4) was solved with zero initial conditions $(x(0) = 0, y(0) = 0)$ with integration step length of 0.005 and a total simulation time; $T_{sim} = 500$. The first 1000 initial iterates were discarded as transients. The response curves are generated while varying other system parameters to represent the variation of the response amplitude with respect to the high-frequency signal's amplitude.

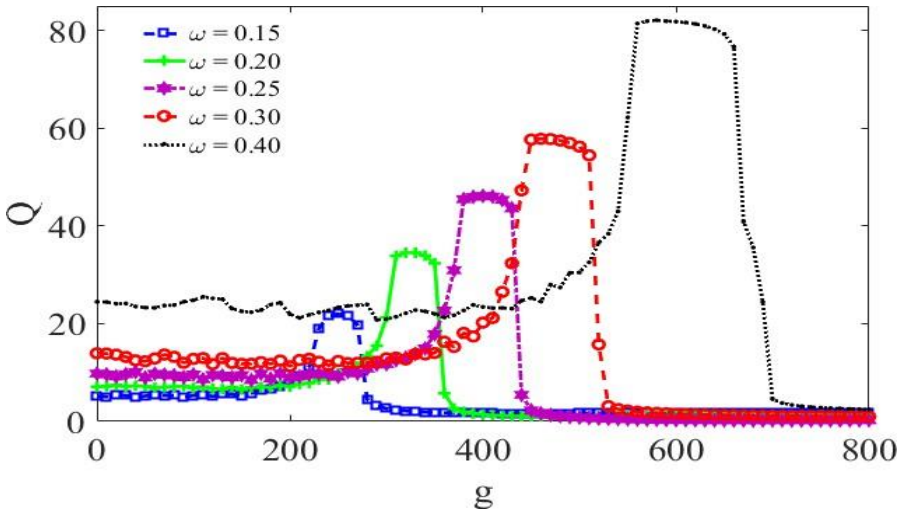

Figure 1: Resonant Curves (Response amplitude, *Q* versus HF amplitude, *g*) for different values of the low-frequency, ω = [0.15, 0.20, 0.25, 0.30, 0.40]

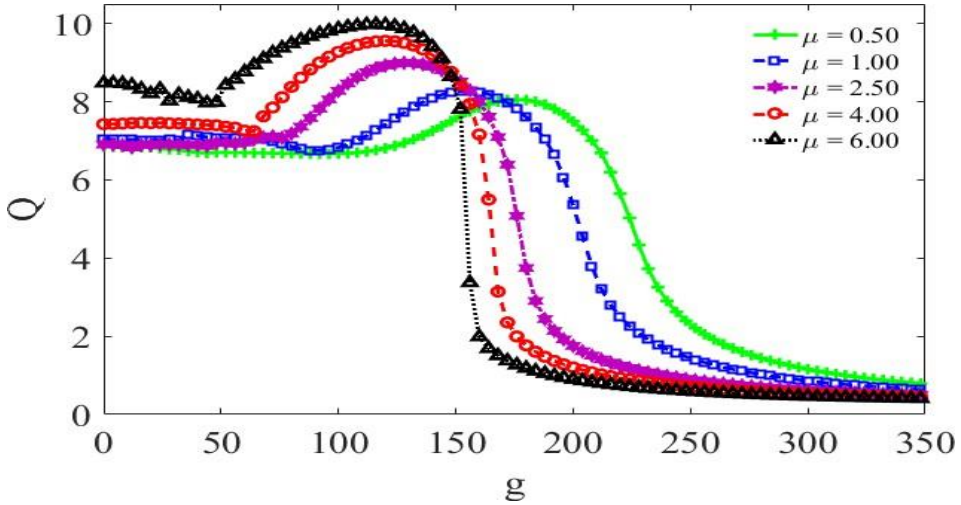

Figure 2: Resonant Curves (Response amplitude *Q* versus HF amplitude, *g*) for different values of the damping coefficient, μ = [0.50, 1.00, 2.50, 4.00, 6.00]. the parameter-induced resonance showed significant difference in behaviour from the traditional vibrational resonance as can be observed in Figure 1

RESULTS AND DISCUSSION

The occurrence of vibrational resonance was confirmed with response curves for the variation of response amplitude, Q with HF amplitude, g for different values of other system parameters as shown in Figures 1 - 6. From the resonant curves, single peak resonances which are amenable to parameter modulation were observed. Parameter modulation of system phenomena is a necessary tool for control and prediction.

Figure 1 shows the effects of low-frequency (LF) modulation on the observed single-peak resonance for the variation of response amplitude with HF g for five values of the LF ω = [0.15, 2.0, 2.5, 3.0, 4.0]. The system's response is amplified as the value of LF, ω rises, hence increasing the value of HF amplitude, g, at the highest resonance, $g_{V\,R}$. As may be seen in Figures 4.9 and 4.10, respectively, the maximum response amplitude, or Q_{ma}, increases as LF, ω, and damping coefficient, μ, rise. However, Figure 2 shows $g_{V\,R}$ reduces with increasing damping coefficient, μ. The role of nonlinear damping coefficient is consistent with established results of (Roy-Layinde et al., 2017), where nonlinear dissipation in form of frictional inhomogeneity was shown to cooperate with the parameters of the fast signal to control vibrational resonant state in a bi-harmonically driven inhomogeneous system defined by nonuniform spatial damping and a periodic potential.

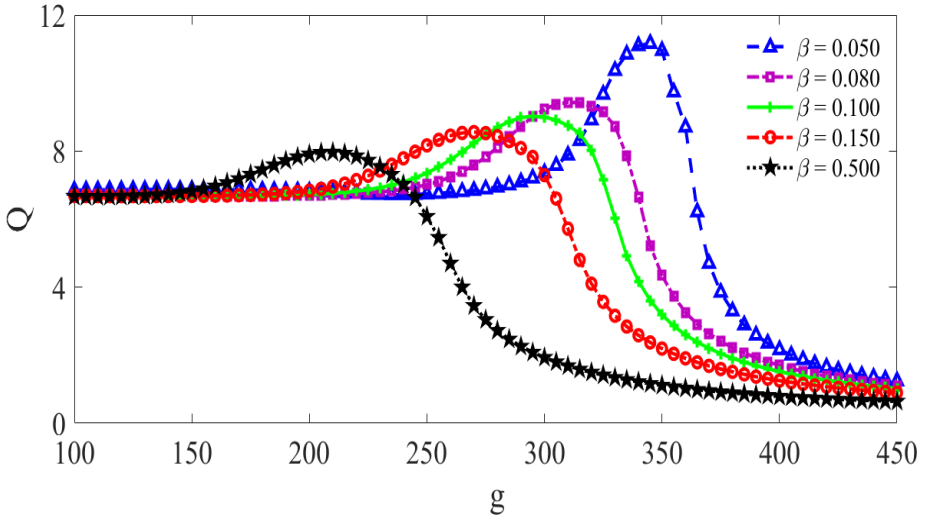

Figure 3: Resonant Curves (Response amplitude Q versus HF amplitude, g) for different values of the nonlinear damping parameter β = [0.050, 0.080, 0.100, 0.150, 0.500]

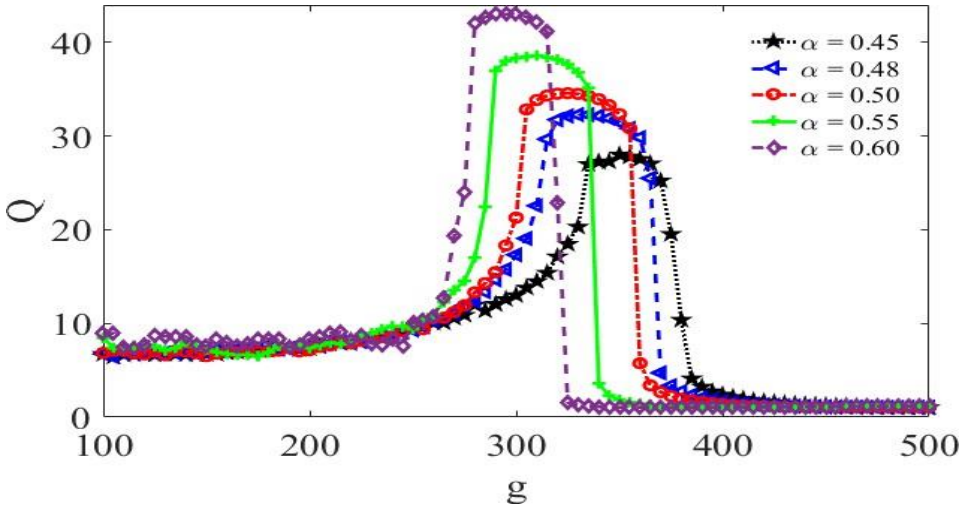

Figure 4: Resonant Curves (Response amplitude, Q versus HF amplitude, g) for different values of the system parameter, α = [0.45, 0.48, 0.50, 0.55, 0.60]

Next, we showed that the control of observed resonances earlier achieved through the damping coefficient as shown in Figure 2 can be achieved through the damping nonlinearities β and α. This is shown Figure 3 and Figure 4 for the variation of response amplitude Q with HF amplitude for different values of the nonlinearities β and α, respectively. Figure 3 shows increase in β = [0.05, 0.08, 0.10, 0.15, 0.50] reduces both Q_{max} and $g_{V\,R}$ for the observed single-peak resonance curves. Hence increase in β leads to suppression and the maximum response occurs at lower value of HF amplitude. Figure 4 depicts the variation of response amplitude with respect to the HF amplitude g for five values of α = [0.45, 0.48, 0.50, 0.55, 0.60]. The resonance curves are shifted towards the left with higher Q_{max} occurring at lower $g_{V\,R}$ as α increases. It can be deduced that increasing α leads to enhancement at lower value of HF amplitude. Hence a combined modulation of both damping nonlinearities can also be used to control the basic features of observed single-peak resonances.

The occurrence VR and control of observed resonance is shown in Figure 5 of the variation of the response amplitude Q with respect to the HF amplitude g for different values of HF Ω = [40ω, 50ω, 60ω, 70ω, 80ω, 90ω]. Evidently, the resonance peaks are enhanced by increasing the high-frequency. Also the peaks occur at higher values of HF amplitude $g_{V\,R}$. However, only the maximum response Q_{max} can be controlled by varying the amplitude of the low-frequency signal f , $g_{V\,R}$ is not significantly changed as observed in Figure 6.

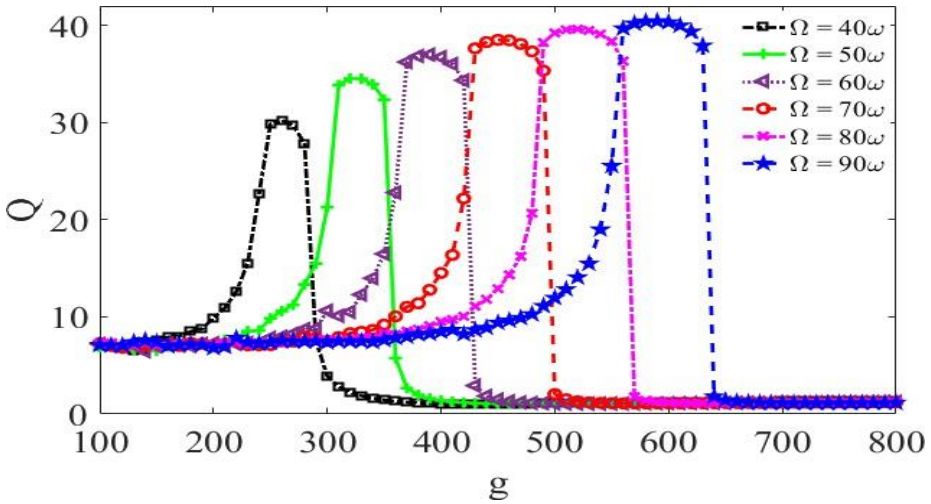

Figure 5: Resonant Curves (Response amplitude, Q versus HF amplitude, g) for different values of the frequency of the HF signal, Ω = [40ω, 50ω, 60ω, 70ω, 80ω, 90ω]

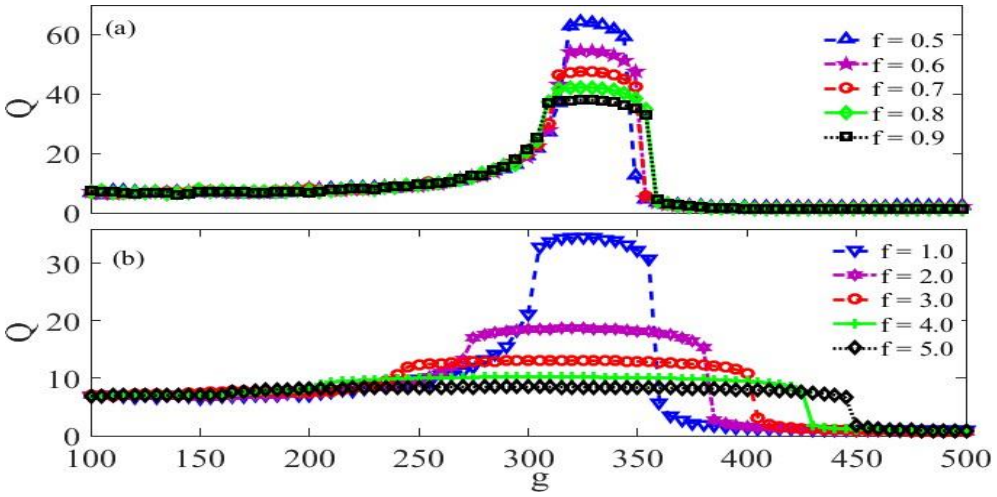

Figure 6: Resonant Curves (Response amplitude, Q versus HF amplitude, g) for different values of the amplitude of the LF signal, (a) f = [0.5, 0.6, 0.7, 0.8, 0.9], (b) f = [1.0, 2.0, 3.0, 4.0, 5.0]

Next, we discuss the possibility of initiating resonance through the cooperation of the HF signal parameters and the damping coefficient. Traditionally, VR is initiated by the parameters on the HF signal. However, it has been shown that other system parameters can induce resonance in the presence of the HF signal (Usama et al., 2019; Roy-Layinde et al., 2022). Figures 7 - 12 show nonconventional resonances can be induced by the damping coefficient μ. The figures depict the response amplitude Q as a function of the damping coefficient μ for different values of other system parameters.

The single peak resonance VR observed for the variation of HF amplitude g can also be induced from the variation of damping coefficient μ as shown in Figure 7 for different values of HF amplitude g, Figures 8 and 9 for different nonlinearities β and α, respectively and in Figures 10 and 11 for different low-frequency parameters ω and f , respectively. For all cases within the parameter regime, the system displayed a resonance peak which is controllable by the values of an amendable system parameter while keeping other parameters constant.

Figure 7 depicts the resonance curves induced by the variation of the damping coefficient for four values of the HF amplitude g = [90, 100, 120, 130]. Only single peak resonances were realized for all values of HF amplitude g chosen within the resonant regime. However, the HF amplitude increases the value of the damping coefficient at which the system response is maximized. This implies the features of the unconventional resonance realised can be controlled by the HF signal parameter. Also, both nonlinear damping parameters β and α can be used to change Q_{max} and μ_{VR}. Figure 8 shows that Q_{max} is reduced with increasing nonlinearity β. In Figure 9, when β is constant, the ther damping nonlinearity shows significant enhancement when increased through α = [0.10, 0.30, 0.50, 0.80, 1.00].

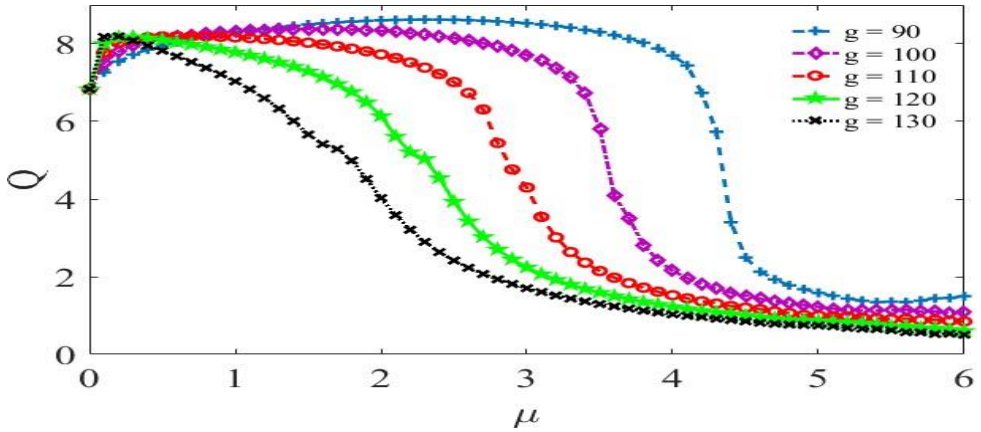

Figure 7: Resonant Curves (Response amplitude Q versus the parameter of the system, μ) for different values of the amplitude of the HF signal, g = [90, 100, 110, 120, 130]

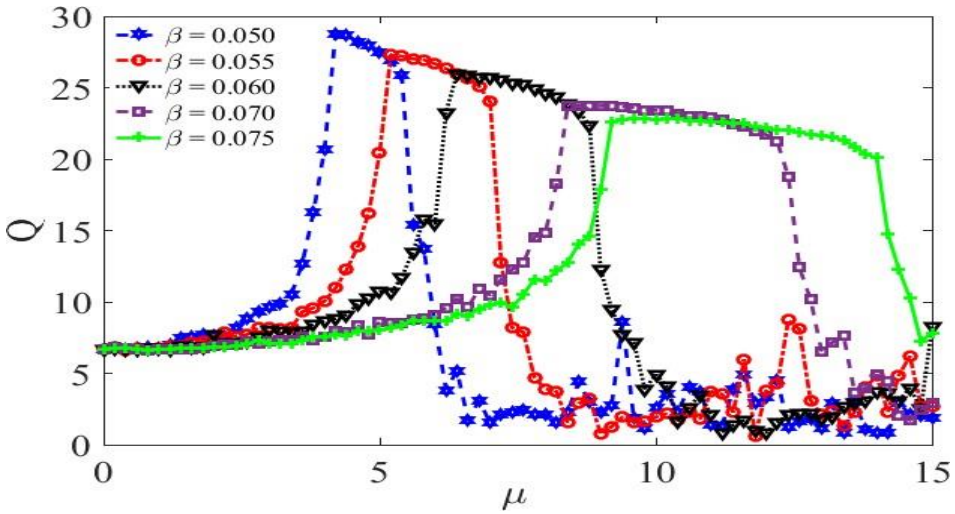

Figure 8: Resonant Curves (Response amplitude Q versus a parameter of the system, μ) for different values of the system parameter, β = [0.050, 0.055, 0.060, 0.070, 0.075]

The parameters of the LF signal, ω and f can also be used to control the observed damping-induced VR. Figure 10 shows the resonant curves for different low-frequecy values ω = [0.20, 0.22, 0.24, 0.25, 0.26]. By increasing the low-frequecy, the system's response is enhanced with obvious increment in the computed maximum response amplitude Q_{max} and the of μ where resonance occur μ_{VR}. Also, similar level control can be achieved by changing the values of the LF amplitude f as shown in Figure 11 for five values of f = [0.10, 0.30, 0.50, 0.80, 1.00]. Figure 12 shows the possibility of enhancement of observed peaks from higher values of f. The damping-induced resonances are shown in Figure 13(a) - (d) for four values of LF (a) ω = 0.15, (b) ω = 0.20, (c) ω = 0.25, and (d) ω = 0.30. Single-peak resonance curve is observed in Figure 13(a). Increasing the LF enhances observed resonance as depicted by the clear increase in maximum response amplitude Q_{max} for increased ω as shown in Figure 13(a) -(d). Also, the value of the damping coefficient at which response is maximized is reduced with increased ω. Interestingly, increase in the LF also initiates other suppressed peaks as shown Figure 13(b)-(d). The observed suppressed peaks suggest the possibility of recovering multiple peaks if other parameters are modulated within its resonant regimes. This is executed as depicted in Figure 14 by varying the HF amplitude g within the regimes of Figure 13(b) to induce double-resonance.

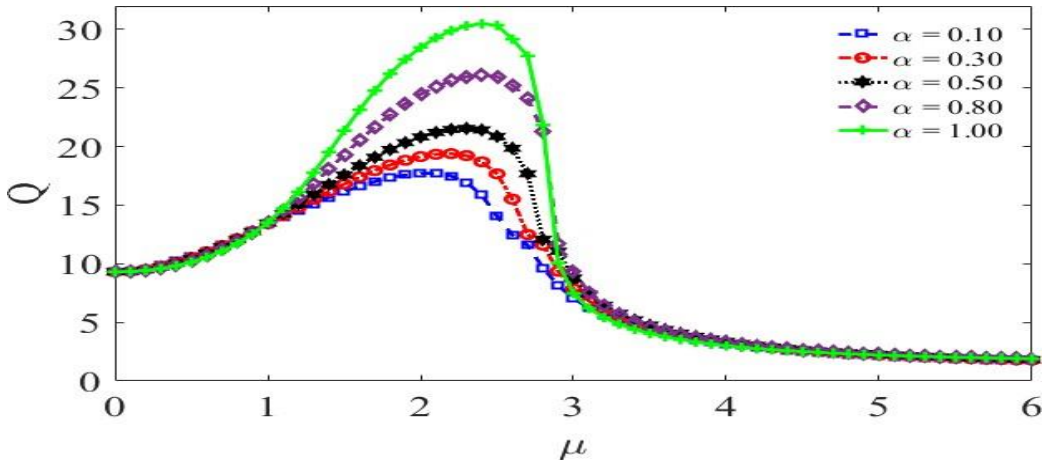

Figure 9: Resonant Curves (Response amplitude Q versus the parameter of the system, μ) for different values of the system's parameter, α = [0.10, 0.30, 0.50, 0.80, 1.00]

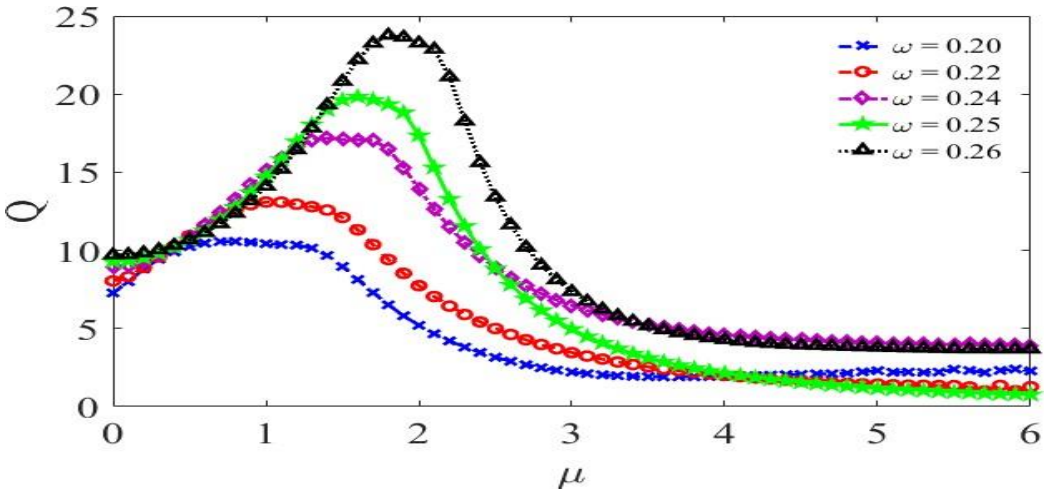

Figure 10: Resonant Curves (Response amplitude Q versus the parameter of the system, μ) for different values of the frequency of the LF signal, ω = [0.20, 0.22, 0.24, 0.25, 0.26]

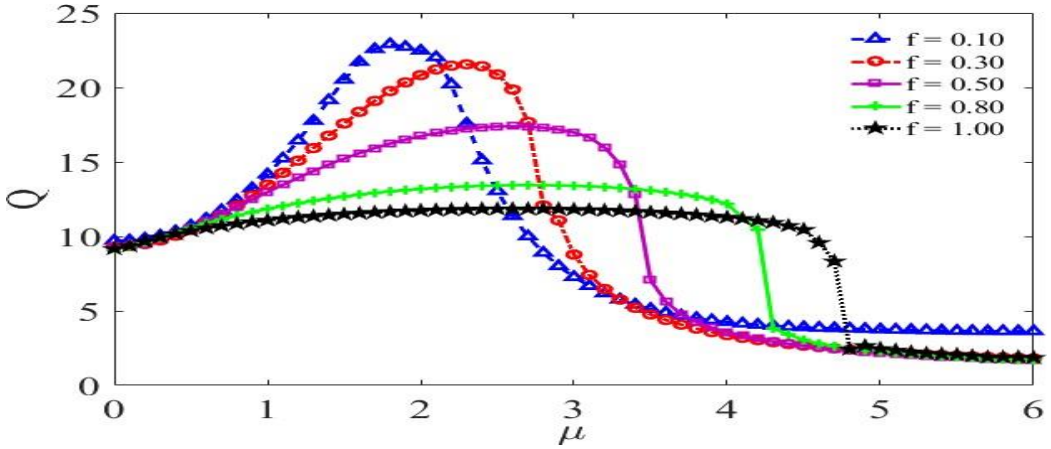

Figure 11: Resonant Curves (Response amplitude Q versus the parameter of the system, μ) for different values of the amplitude of the LF signal, f = [0.10, 0.30, 0.50, 0.80, 1.00]

Figure 14 shows that the damping coefficient can induce both single resonance (Figure 14(a)) and double resonance (Figure 14(d)) when the HF amplitude is varied. The enhancement and development of the suppressed peak into another peak for the emergence of double resonance is shown through Figure 14(a)-(d) for (a) g = 100, (b) g = 150, (c) g = 170, and (d) g = 190. Considering the above, it is necessary to state that the damping coefficient has been shown to control VR (see Figure 3), induce resonance (see Figure 13) and importantly, cooperate with the HF amplitude to lead the system from single to double resonances as shown in Figure 14.

The double resonances or bi-resonance has also been achieved from system parameters like the results produced herein in studies on integer-order systems (Jeyakumari et al., 2009a,b; Yang and Zhu, 2012), fractional-order systems (Calim et al., 2021), biological system (Fu et al., 2022) and systems with variable mass (Roy-Layinde et al., 2022). Variable mass parameters have an influence on the resonance characteristics in a VR research using a system with variable position-dependent mass by causing the system to transition from single resonance to double resonance (Roy-Layinde et al., 2022). When systems are not driven deterministically, double vibrations can occur. Double stochastic resonance (DSR) is the term for the phenomena that has been reported to occur in systems driven by noise (Qiao et al., 2021).

The nonlinearity can control the damping-induced resonance as shown in Figure 8 for the variation of the response amplitude Q with respect to the damping coefficient μ for different values of the nonlinearity β = [0.050, 0.055, 0.060, 0.070, 0.075]. The peak and value of damping coefficient at which resonance occur can be controlled by the nonlinear parameter β. Also, the the low-frequency signal amplitude f controls the response curve – Q *vs*μ, similarly shown in Figure 12 to its role in controlling observed Q *vs* g resonances in Figure 6.

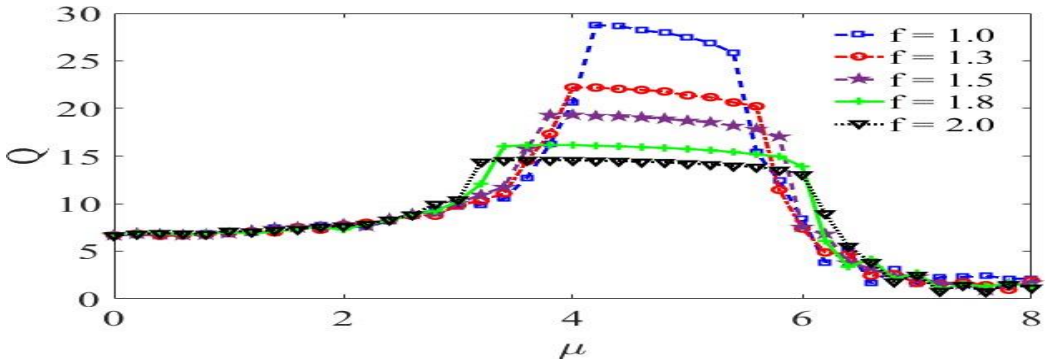

Figure 12: Resonant Curves (Response amplitude Q versus a parameter of the system, μ) for different values of the amplitude of the LF signal, f = [1.0, 1.3, 1.5, 1.8, 2.0]

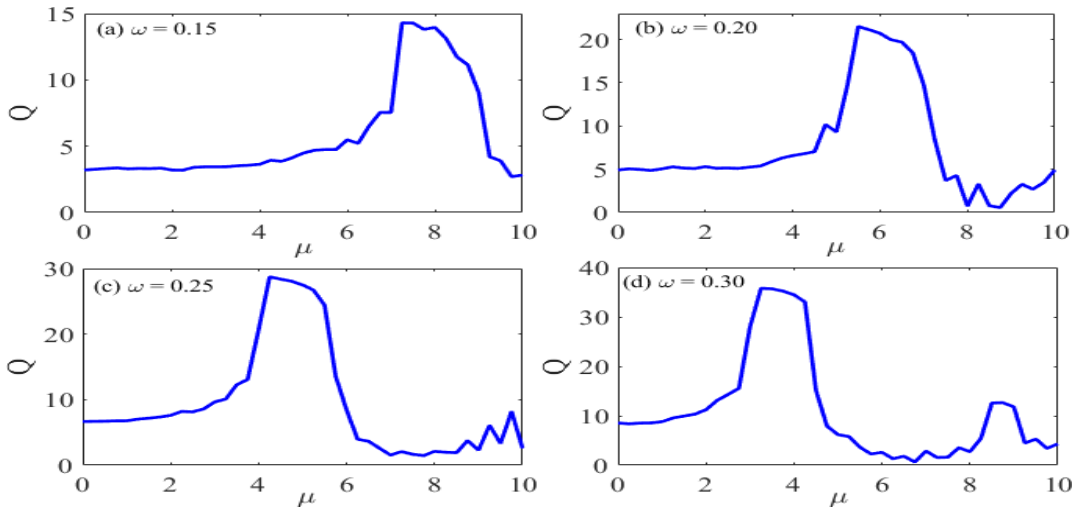

Figure 13: Resonant Curves (Response amplitude Q versus a parameter of the system, μ) for different values of the amplitude of the LF signal, (a) ω = 0.15, (b) ω = 0.20, (c) ω = 0.25, (d) ω = 0.30

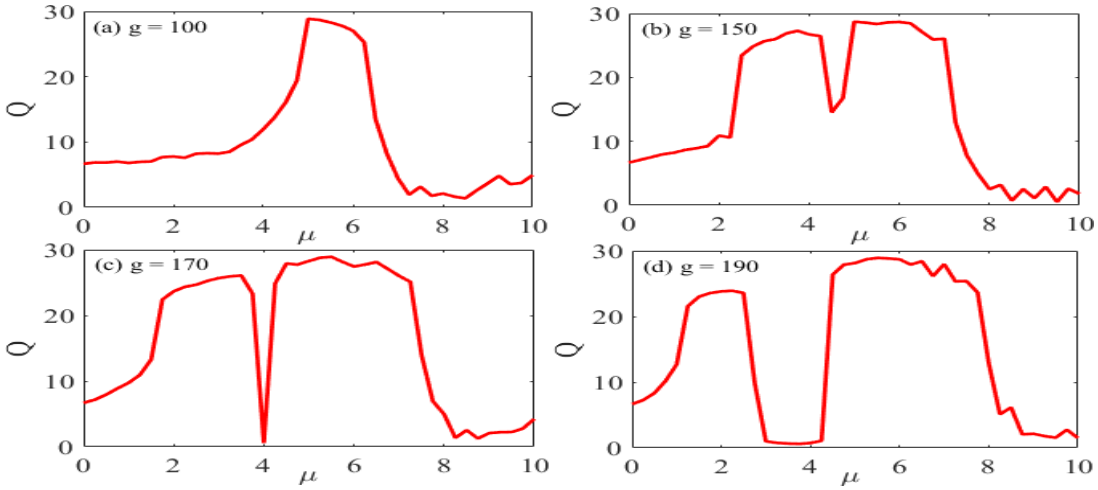

Figure 14: Resonant Curves (Response amplitude Q versus a parameter of the system, μ) for different values of the amplitude of the HF signal, (a) g = 100, (b) g = 150, (c) g = 170, (d) g = 190

CONCLUSION

Vibrational resonance phenomenon was established in the biophysical system from numerical computation of response amplitude by qualitatively describing the response curves obtained from the computation of the response amplitude as a function of the high-frequency amplitude and the damping coefficient. The response curves computed from the response amplitudes exhibited a series of peaks denoting resonance as the frequency or the amplitude of the high-frequency input was varied. Single peak resonances which were amenable to variation of other system parameters were reported. The damping coefficient induced resonance single and double resonances in by cooperating with the parameters of the high-frequency input signal. The induced resonance could lead to significant brain wave activity related to inherent energy transfers from changes to the decay rate, and enzyme-substrate combination, and could be observed from the Electroencephalogram.

REFERENCES

Calim, A., Palabas, T., and Uzuntarla, M. (2021). Stochastic and vibrational resonance in complex networks of neurons. *Philosophical Transactions of the Royal Society A*, 379(2198):20200236.

Chizhevsky, V. (2021). Amplification of optical signals in a bistable vertical-cavity surface-emitting laser by vibrational resonance. *Philosophical Transactions of the Royal Society A*, 379(2192):20200241.

Chizhevsky, V. N. (2014). Experimental evidence of vibrational resonance in a multistable system. *Physical Review E*, 89:062914.

Chizhevsky, V. N. and Giacomelli, G. (2006). Experimental and theoretical study of vibrational resonance in a bistable system with asymmetry. *Physical Review E*, 73(2):022103.

Fr o¨hlich, H. (1968). Long range coherence and energy storage in biological systems. International Journal of Quantum Chemistry, 2:641-649.

Fu, P., Wang, C.-J., Yang, K.-L., Li, X.-B., and Yu, B. (2022). Reentrance-like vibrational resonance in a fractional-order birhythmic biological system. Chaos, Solitons and Fractals, 155:111649.

Gitterman, M. (2001). Bistable oscillator driven by two periodic fields. *Journal of Physics A: Mathematical and General*, 34(24):L355.

Jeyakumari, S., Chinnathambi, V., Rajasekar, S., and Sanjua´n, M. A. (2011). Vibrational resonance in an asymmetric duffing oscillator. *International Journal of Bifurcation and Chaos*, 21(01):275–286.

Jeyakumari, S., Chinnathambi, V., Rajasekar, S., and Sanjuan, M. A. F. (2009a). Analysis of vibrational resonance in a quintic oscillator. *Chaos: An Interdisciplinary Journal of Nonlinear Science*, 19(4):043128.

Jeyakumari, S., Chinnathambi, V., Rajasekar, S., and Sanjuan, M. A. F. (2009b). Single and multiple vibrational resonance in a quintic oscillator with monostable potentials. *Physical Review E*, 80(4):046608.

Kadji, H. E., Orou, J. C., Yamapi, R., and Woafo, P. (2007). Nonlinear dynamics and strange attractors in the biological system. *Chaos, Solitons and Fractals*, 32(2):862–882.

Kaiser, F. (1981a). *Coherent excitations in biological systems: specific effects in externally driven self-sustained oscillating biophysical systems*. Springer-Verlag, Berlin, Heidelberg.

Kaiser, F. (1981b). Coherent modes in biological systems. *Biological effects of nonionizing radiation*, 157:219.

Kaiser, F. and Eichwald, C. (1991). Bifurcation structure of a driven, multi-limit-cycle van der pol oscillator (i): The superharmonic resonance structure. *International Journal of Bifurcation and Chaos*, 1(02):485–491.

Morfu, S., Usama, B., and Marquie´, P. (2021). On some applications of vibrational resonance on noisy image perception: the role of the perturbation parameters. *Philosophical Transactions of the Royal Society A*, 379(2198):20200240.

Olusola, O., Shomotun, O., Vincent, U., and McClintock, P. (2020). Quantum vibrational resonance in a dual-frequency-driven Tietz-Hua quantum well. *Physical Review E*, 101(5):052216.

Omoteso, K. A., Roy-Layinde, T. O., Laoye, J. A., Vincent, U. E., and McClintock, P. V. E. (2021). Acoustic vibrational resonance in a Rayleigh-Plesset bubble oscillator. *Ultrasonics Sonochemistry*, 70:105346.

Oyeleke K., Olusola, O., Vincent, U. E., Ghosh, D., and McClintock, P. V. (2021). Parametric vibrational resonance in a gyroscope driven by dual-frequency forces. *Physics Letters A*, 387:127040.

Pan, Y., Duan, F., Chapeau-Blondeau, F., Xu, L., and Abbott, D. (2021). Study of vibrational resonance in nonlinear signal processing. *Philosophical Transactions of the Royal Society A*, 379(2192):20200235.

Paul, S. and Shankar Ray, D. (2021). Vibrational resonance in a driven two-level quantum system, linear and nonlinear response. *Philosophical Transactions of the Royal Society A*, 379(2192):20200231.

Pereira, C. (2015). Biophysical understanding of resonance at a cellular level. Journal of Metaphysics and Connected Consciousness Vol, 1:1–3.

Qiao, Z., Liu, J., Ma, X., and Liu, J. (2021). Double stochastic resonance induced by varying potential-well depth and width. *Journal of the Franklin Institute*, 358(3):2194–2211.

Qin, T., Xie, T., Luo, M., and Deng, K. (2017). Vibrational resonance in fractional-order overdamped multistable systems. *Chinese Journal of Physics*, 55(2):546–555.

Rajaseker, S., Abirami, K., and Sanjua´n, M. A. F. (2011). Novel vibrational resonance in multistable systems. *Chaos*, 21(3):033106.

Rajasekar, S. and Sanjuan, M. A. (2016). Nonlinear resonances. Springer.

Roy-Layinde, T. O., Laoye, J. A., Popoola, O. O., and Vincent, U. E. (2016). Analysis of vibrational resonance in bi-harmonically driven plasma. *Chaos*, 26(9):093117.

Roy-Layinde, T. O., Laoye, J. A., Popoola, O. O., Vincent, U. E., and McClintock, P. V. E. (2017). Vibrational resonance in an inhomogeneous medium with periodic dissipation. *Physical Review E*, 96:032209.

Roy-Layinde, T. O., Omoteso, K. A., Ogooluwa, D. O., Oladunjoye, H. T., and Laoye, J. A. (2020). Chaotic and periodic behavior in a fractional-order biological system. Acta Physica Polonica B, 51(9):1885-1904.

Roy-Layinde, T. O., Omoteso, K. A., Oyero, B. A., Laoye, J. A., and Vincent, U. E. (2022). Vibrational resonance of ammonia molecule with doubly singular position-dependent mass. *The European Physical Journal B*, 95(5):1–11.

Roy-Layinde, T. O., Omoteso, K. A., Diala, U. H., Runsewe, J. A., and Laoye, J. A. (2024). Analysis of vibrational resonance in an oscillator with exponential mass variation. *Chaos, Solitons and Fractals, 178*, 114310.

Sahoo, P. K. and Chatterjee, S. (2021). High-frequency vibrational control of principal parametric resonance of a nonlinear cantilever beam: Theory and experiment. *Journal of Sound and Vibration*, 505:116138.

Usama, B. I., Morfu, S., and Marquie´, P. (2019). Numerical analyses of the vibrational resonance occurrence in a nonlinear dissipative system. *Chaos, Solitons and Fractals*, 127:31–37.

Vincent, U. E., Roy-Layinde, T. O., Adesina, P. O., Popoola, O. O., and McClintock, P. V. E. (2018). Vibrational resonance in an oscillator with an asymmetrical deformable potential. *Physical Review E*, 98:062203.

Vincent, U. E., McClintock, P. V., Khovanov, I., and Rajasekar, S. (2021). Vibrational and stochastic resonances in driven nonlinear systems.

Yan, Z., Wang, W., and Liu, X. (2018). Analysis of a quintic system with fractional damping in the presence of vibrational resonance. *Applied Mathematics and Computation*, 321:780–793.

Yang J. H. and Liu, X. B. (2010). Controlling vibrational resonance in a multistable system by time delay. *Chaos*, 20(3):033124.

Yang, W. (2012). Positive solutions for a coupled system of nonlinear fractional differential equations with integral boundary conditions. *Computational and Applied Mathematics*, 63:288–297.

Yang, J., Rajasekar, S., and Sanjuán, M. A. (2024). Vibrational resonance: A review. Physics Reports, 1067, 1-62.

Yao, C. and Zhan, M. (2010). Signal transmission by vibrational resonance in one-way coupled bistable systems. *Physical Review E*, 81(6):061129.

Yu, H., Wang, J., Liu, C., Deng, B., and Wei, X. (2011). Vibrational resonance in excitable neuronal systems. *Chaos: An Interdisciplinary Journal of Nonlinear Science*, 21(4):043101.